

Accepted to ApJ Letters 2008 April 17

## Dead Zone Accretion Flows in Protostellar Disks

N. J. Turner<sup>1</sup> and T. Sano<sup>2</sup>

### ABSTRACT

Planets form inside protostellar disks in a dead zone where the electrical resistivity of the gas is too high for magnetic forces to drive turbulence. We show that much of the dead zone nevertheless is active and flows toward the star while smooth, large-scale magnetic fields transfer the orbital angular momentum radially outward. Stellar X-ray and radionuclide ionization sustain a weak coupling of the dead zone gas to the magnetic fields, despite the rapid recombination of free charges on dust grains. Net radial magnetic fields are generated in the magneto-rotational turbulence in the electrically conducting top and bottom surface layers of the disk, and reach the midplane by Ohmic diffusion. A toroidal component to the fields is produced near the midplane by the orbital shear. The process is similar to the magnetization of the Solar tachocline. The result is a laminar, magnetically-driven accretion flow in the region where the planets form.

*Subject headings:* circumstellar matter — solar system: formation — stars: formation — instabilities — MHD

### 1. INTRODUCTION

The planets of Sun-like stars form from a protostellar disk consisting of 0.01–0.1 Solar masses of gas together with 1% dust by mass. The removal of orbital angular momentum from the disk is a key to understanding the origins of the planets as it determines the rate at which material spirals in to accrete on the star. The magneto-rotational instability or MRI (Balbus & Hawley 1991) transfers angular momentum outward and taps the free energy in the differential orbital rotation of the disk to drive turbulence and regenerate magnetic fields,

---

<sup>1</sup>Jet Propulsion Laboratory, California Institute of Technology, Pasadena, California 91109, USA; neal.turner@jpl.nasa.gov

<sup>2</sup>Institute of Laser Engineering, Osaka University, Suita, Osaka 565-0871, Japan; sano@ile.osaka-u.ac.jp

at locations where the gas is sufficiently ionized to couple strongly to the fields. However the minimum-mass protosolar disk, constructed by adding sufficient hydrogen and helium to the planets to give Solar composition (Hayashi et al. 1985), is mostly too cold for thermal ionization. The minimum-mass disk has surface mass density  $\Sigma = 1700(r/\text{AU})^{-3/2} \text{ g cm}^{-2}$  and temperature  $T = 280(r/\text{AU})^{-1/2} \text{ K}$  at radius  $r$  measured in astronomical units (AU), and is in vertical hydrostatic balance. Cosmic rays and stellar coronal X-rays are absorbed before reaching the midplane, and ionize only the surface layers. Furthermore, rapid recombination on grain surfaces leads to low abundances of the free electrons otherwise responsible for most of the conductivity. Consequently, much of the region where the planets form is not subject to the MRI. The region consists of a laminar resistive interior sandwiched between two conducting surface layers where magneto-rotational turbulence causes an accretion flow (Gammie 1996; Sano et al. 2000; Fromang et al. 2002; Ilgner & Nelson 2006). The interior is not completely quiescent, as waves propagating from the turbulent layers cause hydrodynamic stresses and low rates of accretion (Fleming & Stone 2003). Magnetic stresses can occur in the interior under favorable conditions, if small grains are removed, for example by incorporation into planetesimals, and ionizing cosmic rays reach the disk unimpeded by the stellar wind (Turner et al. 2007). However, the resistive interior of the disk retains a weak coupling to the magnetic fields even if grains are present and cosmic rays are absent. The weak coupling is the topic of this paper.

## 2. CRITERION FOR SHEAR-GENERATED MAGNETIC FIELDS

Magnetic forces can extract angular momentum from the gas if the fields have both toroidal and poloidal components. We derive a criterion for the generation of toroidal fields by shear acting on radial fields. The Ohmic diffusion quickly eliminates any vertical magnetic gradients in the resistive layer, while the conducting layers above and below prevent the fields from escaping. The resistive layer can be approximated by an axisymmetric cylindrical flow in Keplerian rotation with a uniform resistivity  $\eta$ . The toroidal component of the induction equation reduces to  $\partial B_\phi / \partial t = -\frac{3}{2}\Omega B_r + \eta(\nabla^2 B_\phi - B_\phi/r^2)$  where  $B_r$  and  $B_\phi$  are the radial and toroidal field components in cylindrical coordinates and  $\Omega$  is the orbital frequency. If also the toroidal field varies as a power-law with radius,  $B_\phi \sim r^p$ , the field grows through the shear term provided  $r^2\Omega/\eta > \frac{2}{3}(p^2 - 1)B_\phi/B_r$ . We consider the implications for the minimum-mass protosolar disk. The magnetic pressure is unlikely to exceed the midplane gas pressure, owing to the buoyancy of the fields. The magnetic pressure is a fixed fraction of the midplane gas pressure if the power-law index  $p = -13/8$ . The resulting criterion for shear-generated toroidal fields to grow to about ten times the radial seed field strength,

$$v_\phi^2/(\eta\Omega) > 10, \quad (1)$$

resembles the criterion (Sano & Stone 2002) for magneto-rotational turbulence  $v_{Az}^2/(\eta\Omega) > 1$ . However the shear criterion equation 1 allows magnetic activity at far greater resistivities, since the flattened shape of the disk requires an orbital speed  $v_\phi$  much greater than the sound speed  $c_s$ , which in turn is typically greater than the vertical Alfvén speed  $v_{Az}$ . The orbital speed is a few hundred times the vertical Alfvén speeds found at the midplane in numerical calculations of magneto-rotational turbulence (Miller & Stone 2000). The part of the dead zone where the shear criterion holds is better named the “undead zone” because it can be reactivated by radial fields siphoned off from the adjacent turbulent layers. In contrast with models where angular momentum is removed from the top and bottom surfaces of the disk by a magneto-centrifugal wind (Blandford & Payne 1982; Wardle & Königl 1993), here the torques arise from locally-generated magnetic fields.

### 3. RESISTIVITY OF THE PROTOSOLAR DISK

The minimum-mass protosolar disk with well-mixed micron-sized grains has an equilibrium resistivity low enough for magneto-rotational turbulence only in the surface layers, at the radii where most of the planets formed (figure 1). A deeper layer can generate smooth large-scale fields by shear according to equation 1, while the midplane within 5 AU of the star is almost completely decoupled from the fields. If the grains are removed by incorporation into planetary embryos, then turbulence or shear can generate magnetic fields in every part of the disk.

Figure 1 was constructed as follows. The resistivity  $\eta = 234\sqrt{T}/x_e$  cm<sup>2</sup> s<sup>-1</sup> varies inversely with the electron fraction  $x_e = n_e/n_n$ , where  $n_e$  is the electron number density and  $n_n$  the number density of neutrals (Blaes & Balbus 1994). We compute the electron fraction by solving a chemical network including ionization by stellar X-rays (Igea & Glassgold 1999) and <sup>26</sup>Al radionuclide decay, dissociative recombination, charge exchange with metal atoms, and grain surface reactions. The recombination is treated using the reduced reaction network with grains described by Ilgner & Nelson (2006). The fraction of the metal atoms free to enter the gas phase is chosen to be 1%. The resistivity depends only weakly on this fraction. The stellar X-ray ionization rate is taken from a fit to Monte Carlo radiative transfer results including scattering (Igea & Glassgold 1999), scaled to a stellar luminosity  $2 \times 10^{30}$  erg s<sup>-1</sup> in 5 keV thermal X-rays to match young Solar-mass stars observed in the Orion nebula (Garmire et al. 2000). The fitted ionization rate is  $\zeta = 2.6 \times 10^{-15}(r/\text{AU})^{-2}(\exp[-\Sigma_a/8.0 \text{ g cm}^{-2}] + \exp[-\Sigma_b/8.0 \text{ g cm}^{-2}])$  s<sup>-1</sup> where  $\Sigma_a$  and  $\Sigma_b$  are the mass columns lying vertically above and below the point of interest. The fit underestimates the ionization rate at mass columns  $< 1 \text{ g cm}^{-2}$ , with no significant effect on

the locations of the dead and undead zones. The decay of  $^{26}\text{Al}$  in the dust grains yields an ionization rate  $4 \times 10^{-19} \text{ s}^{-1}$  (Stepinski 1992). A fraction 0.1% of the radioactive atoms is placed in the gas phase, giving a low rate of ionization even with grains absent. We neglect cosmic ray ionization owing to uncertainty about the extent to which the interstellar energetic particles are blocked by the wind from the young star.

#### 4. MHD CALCULATIONS

We show results from two 3-D isothermal stratified shearing-box (Hawley et al. 1995; Brandenburg et al. 1995; Stone et al. 1996) MHD calculations of small patches of the minimum-mass protosolar disk using the ZEUS code (Stone & Norman 1992). The first is placed at 5 AU and includes well-mixed 1  $\mu\text{m}$  grains with dust-to-gas mass ratio 1% and a magnetic field with a net vertical component of 6 milligauss. The second is placed at 1 AU and has no grains and a net vertical field of 30 milligauss. The net magnetic fields are weak, with midplane ratios of gas to magnetic pressure  $5 \times 10^4$  and  $3.8 \times 10^5$ , respectively. The presence of the net fields ensures that the fastest-growing mode of the linear MRI is spatially resolved in the calculations. To the net field in both cases is added a part with zero net flux that dissipates readily through reconnection. The vertical component is  $B_0 \sin 2\pi x/L$ , the toroidal component  $B_0 \cos 2\pi x/L$  and the radial component zero, where  $x$  is the radial position and  $L$  the box width. The strength  $B_0$  of the sinusoidal field is 0.1 and 1 Gauss, respectively. The resistivity is calculated using the ionization and chemical network described above except that the X-ray ionization rates are directly interpolated in the Monte Carlo radiative transfer results and the fit discussed above is not used. The resistivity is fixed at its initial equilibrium value at each height in the first run, while the resistivity is allowed to vary in space and time through mixing, ionization and recombination in the second run. In other respects the calculations are identical to our recent work (Turner et al. 2007). In particular, the vertical boundaries lie four density scale heights  $H = c_s/\Omega$  above and below the midplane and are open, allowing magnetic fields to escape leaving the patch of disk with a net radial and toroidal magnetic flux. Among the non-ideal terms in the induction equation, ambipolar diffusion is important outside  $4H$ . The Ohmic resistivity is greater than the Hall resistivity near the midplane at 1 AU while the two are comparable at 5 AU (Wardle 2007). Under these conditions the Ohmic term has the bigger impact on the amplitude of magneto-rotational turbulence (Sano & Stone 2002). Our calculations therefore include only the Ohmic diffusion. The domain extends  $2H$  along the radial direction and  $8H$  along the toroidal direction, and is divided into 32 radial by 64 toroidal by 128 vertical zones.

The two calculations give similar results over 130 orbits. A net radial magnetic field

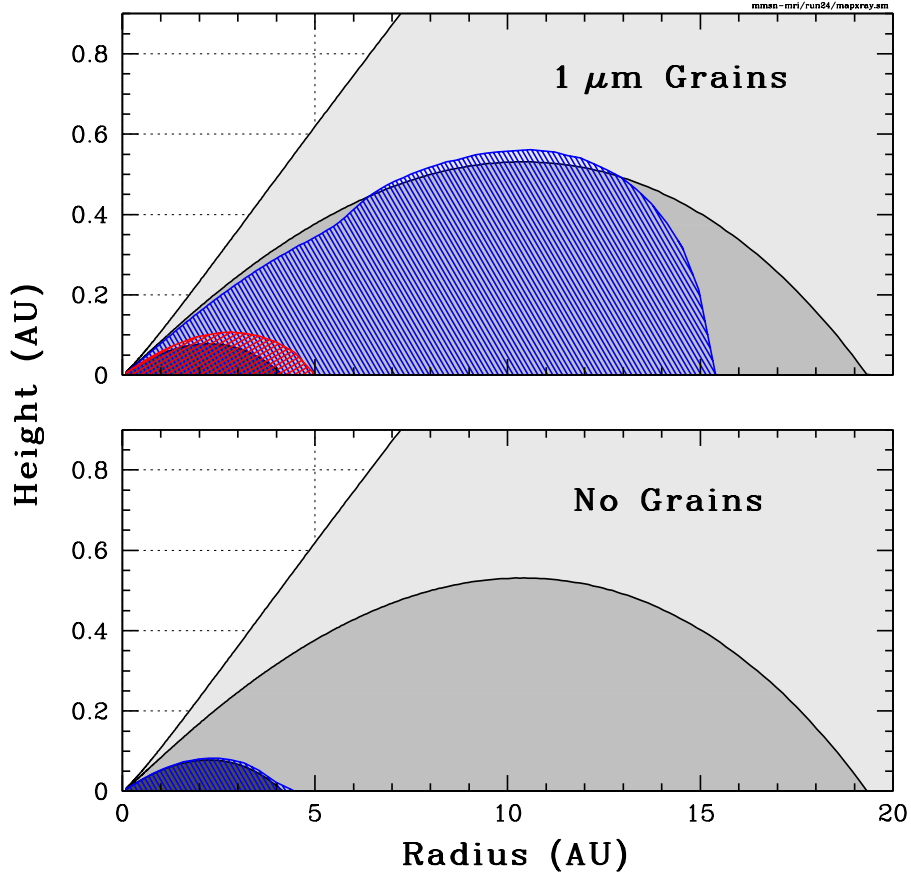


Fig. 1.— Location of the dead zone (red) and undead zone (blue) in a cross-section view of the minimum-mass protosolar disk. The dead zone gas is decoupled from the magnetic fields, while the undead zone is sufficiently ionized for the generation of toroidal fields by shear. The remainder of the disk body is well-coupled to the fields and is turbulent through magnetorotational instability. The star lies at the origin, the disk midplane falls along the horizontal axis, and solid black contours show vertical mass columns of 1, 10 and  $100 \text{ g cm}^{-2}$ . The pressure in the vertical component of the magnetic field is set to 0.1% of the midplane gas pressure. The ionization is due to stellar X-rays and the decay of radioactive  $^{26}\text{Al}$ . Recombination on grain surfaces is included in the calculation shown at top, where the dead zone extends to 5 AU in the midplane. The grains are  $1 \mu\text{m}$  in radius and well-mixed in the gas at a 1% mass fraction. With the grains removed, there is no dead zone (bottom panel).

generated in the turbulent surface layers is mixed to the undead zone where it diffuses to the midplane. The shear in the undead zone generates toroidal fields (figure 2) of the opposite sign, leading to magnetic stresses that transfer angular momentum outward. Lying just

inside the undead zone is a dissipation layer about  $\frac{1}{2}H$  thick that receives magnetic fields when turbulent motions overshoot the edge of the well-coupled gas. The resistivity is too high for magneto-rotational turbulence and dissipates the tangled component of the fields. The Ohmic diffusion time  $H^2/\eta$  at the base of the dissipation layer is about 10 orbits, so that the layer acts as a filter delivering to the undead zone a magnetic field that is a recent time-average of the large-scale field at the edge of the turbulent layer. The radial field in the dissipation layer and at the midplane reverses every 20-50 orbits. The midplane toroidal field changes at approximately the rate  $-\frac{3}{2}\Omega B_r$  due to the shear, indicating that local shear generation dominates other source terms (Turner et al. 2007). The shearing reverses the toroidal field about 10 orbits after the radial field, so that the field lines swing around to trail the rotation and the magnetic stress again becomes positive (figure 3). A related process occurs in the Sun, where magnetic fields generated in the convection zone are carried down to the tachocline and grow there through differential rotation (Parker 1993). The protostellar disk differs in that shear occurs throughout the flow, and the turbulence is shut off by the resistivity of the gas rather than a transition to radiative energy transport.

The resistivity at all heights in the disk is typically unchanged as gas mixes between the surface layers and interior, because the recombination on the grains is fast enough to keep the ionization near its local equilibrium value. However with the grains removed, recombination is slow enough for ionized gas to reach the midplane (Inutsuka & Sano 2005). In our calculation with no grains, the undead zone shrinks after 150 years as ionized gas is carried down from the surface layers. The flow settles after 200 years into a new steady state with an overall accretion rate 20 times greater. The midplane remains magneto-rotationally stable (figure 3).

## 5. EMPIRICAL CONSTRAINTS

The mass flow rate corresponding to the stresses in the MHD calculations (figure 4) is sufficient for the disk to accrete on the star within a few million years, the lifetime inferred from the disk fractions in young star clusters of different ages (Haisch et al. 2001). The magnetic contribution to the stress is several times greater than the hydrodynamic contribution in the dissipation layer, and at times when the fields are strongest in the midplane. The time-averaged midplane magnetic and hydrodynamic contributions are comparable. The undead zone rather than being inactive has a mean mass flow rate 4% to 61% of that in the turbulent layers. The midplane gas moves toward the star on average, but flows away from the star immediately after the reversals in the radial magnetic field when the field lines lead in the rotation. The root-mean-square midplane field strength found in the calculations is

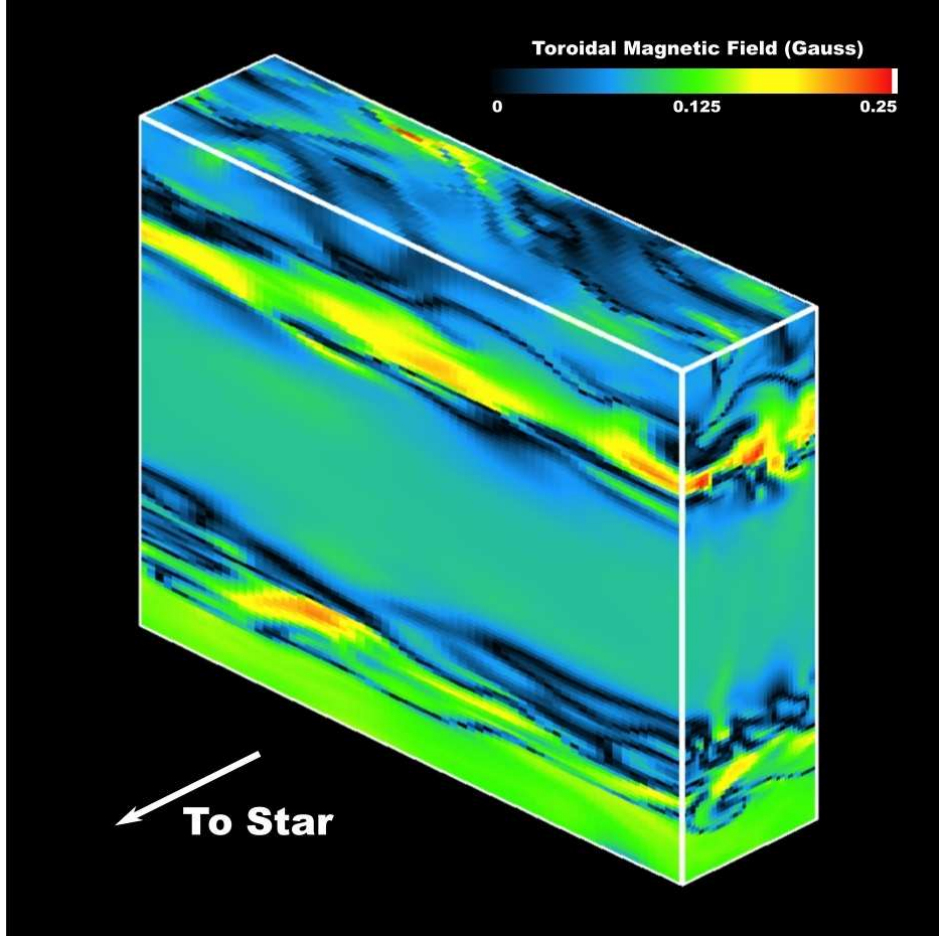


Fig. 2.— Snapshot of the toroidal magnetic field strength at 55 orbits in a resistive MHD calculation of a patch of the protosolar disk at 5 AU including well-mixed  $1 \mu\text{m}$  grains. The undifferentiated zone at center is filled with a uniform, 0.1-Gauss shear-generated toroidal magnetic field while patchy fields are found in the turbulent layers above and below. The star lies off-page to lower left and the disk midplane is horizontal through the image center.

about 0.1 Gauss at 5 AU and 1 Gauss at 1 AU, in the range 0.1–7 Gauss inferred from the relict magnetization of primitive meteorites that were last melted in the asteroid belt during the formation of the Solar system (Cisowski & Hood 1991). The agreement is consistent with the idea that the planet formation region is a laminar, magnetized accretion flow for some part of its history.

The original dead zone picture with a fixed mass column of accreting material (Gammie 1996) yields a unique mass accretion rate approximately  $10^{-8}$  Solar masses per year, independent of the stellar mass. In contrast, observations of T Tauri stars show the accretion

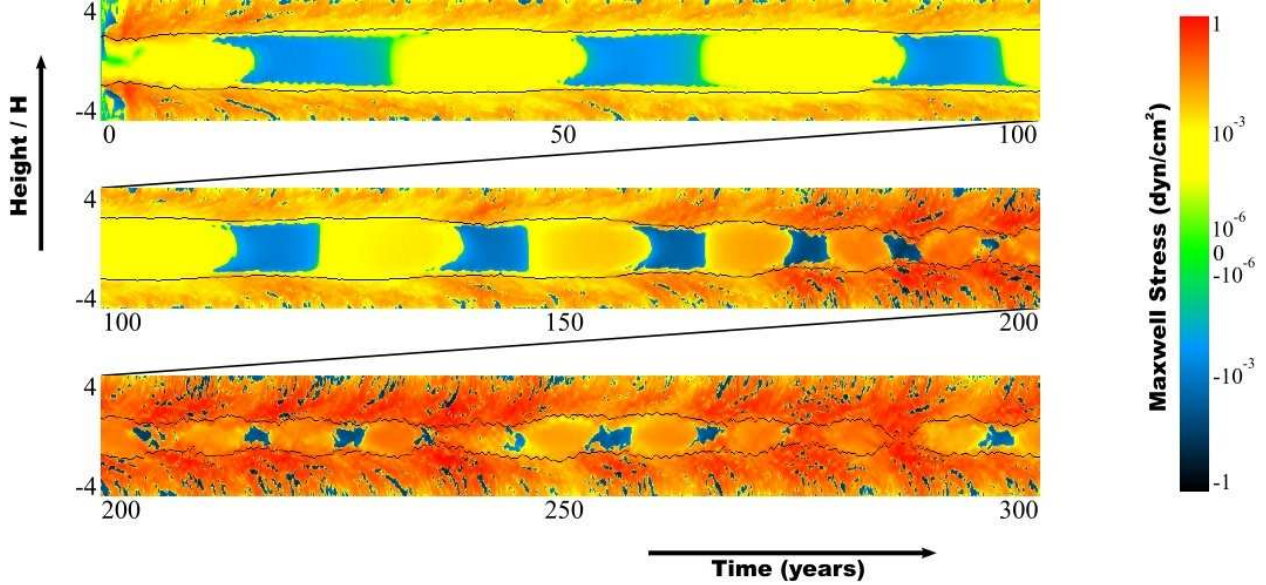


Fig. 3.— Magnetic accretion stress versus height and time in a resistive MHD calculation of a patch of the protosolar disk at 1 AU. The stress is proportional to the radial and toroidal components of the magnetic field. It is horizontally-averaged across the patch and is plotted using a double-logarithmic color scale, with outward angular momentum transport in red and yellow, and inward transport in black and blue. The calculation lasts 300 years and each panel shows a 100-year interval. Black curves mark the edges of the undead zone where the resistivity suppresses magnetorotational turbulence. Magnetic activity in the undead zone is driven by the diffusion of magnetic fields from the turbulent surface layers. After 150 years, the activity grows stronger due to an increase in magnetic coupling as ionized gas is mixed from the surface layers toward the midplane.

rate increases with the stellar mass and has a spread of about two decades at Solar mass (Hartmann et al. 2006). We suggest based on figure 4 that a similar range of accretion rates can be produced by varying the magnetic flux and the abundance of small dust grains.

The radial transport of material over large distances in the early Solar system is indicated by the presence of crystalline silicate grains in Comet 81P/Wild 2 (Brownlee et al. 2006). The crystallization requires temperatures of 1000 K that were found near the Sun, while much of the comet is icy and formed at temperatures below 200 K in the outer Solar system. It remains to be seen whether grains can be carried large radial distances in the turbulent surface layers of the protosolar disk without sinking into the undead and dead zones.

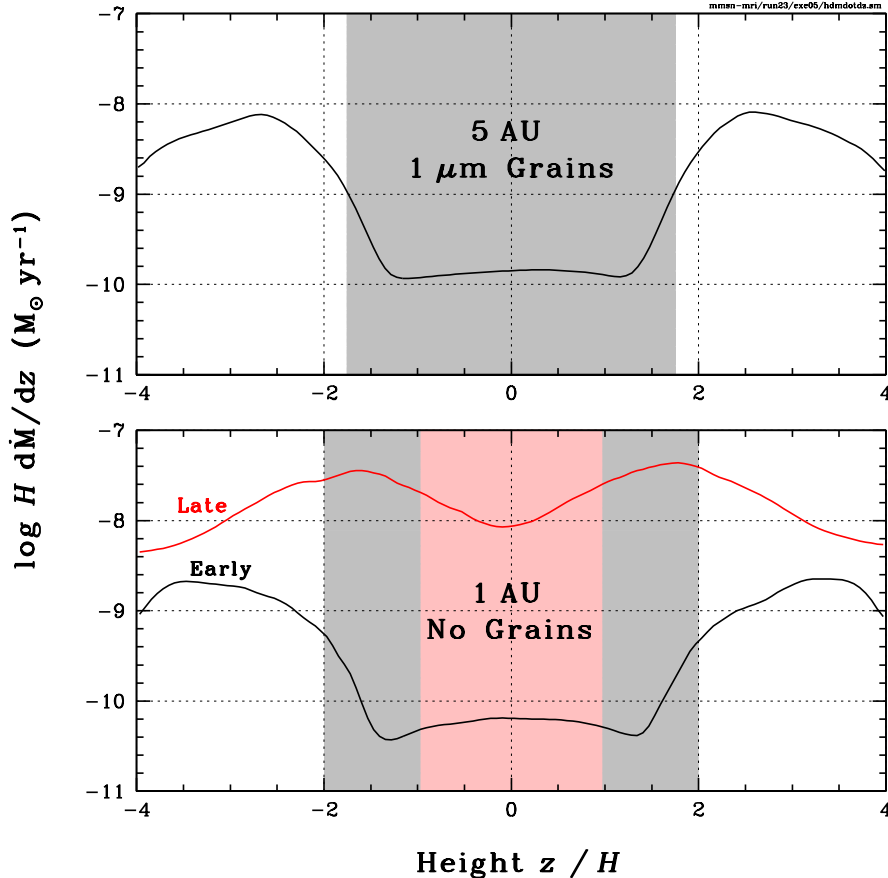


Fig. 4.— Accretion rate corresponding to the total stress in the two MHD calculations located at 5 AU (top) and 1 AU (bottom). The accretion rate per density scale height  $H$  is plotted against the distance  $z$  from the midplane. The results are averaged from 20 to 120 orbits (solid black curves at top and bottom) and after mixing reduces the size of the undead zone, from 200 to 300 orbits (red curve in lower panel). The vertically-integrated accretion rates are  $2.2 \times 10^{-8}$ ,  $6.4 \times 10^{-9}$  and  $1.5 \times 10^{-7}$  Solar masses per year respectively. Shading of the same colors marks the undead zone.

## 6. DISCUSSION

We have found that magnetic stresses control the dead zone evolution even with a full complement of micron-sized grains, in a minimum-mass protosolar disk ionized only by stellar X-rays and radionuclide decay. Consequently, smooth large-scale magnetic fields can occur in a wide range of protostellar disks and drive flows in the dead zone before and during planet formation as well as afterwards.

Models of the early evolution of the solids in protostellar disks depend crucially on the dynamics of the gas and will be affected by the presence of a laminar midplane accretion flow. The gas drag forces in turbulence cause collisions between the particles, leading to the growth or destruction of solid bodies depending on the speeds involved (Dullemond & Dominik 2005). In laminar gas, grains settle toward the midplane on timescales much less than the disk lifetime (Nakagawa et al. 1981). Layered accretion can cause the rapid formation of large bodies as particles colliding in the turbulent surface layers grow large enough to fall into the laminar interior where destructive collisions are rare (Ciesla 2007).

Protoplanets migrate away from the locations where they first formed, by exchanging orbital angular momentum with the disk gas through gravitational torques (Goldreich & Tremaine 1979; Ward 1997). The rapid sunward migration of the cores of Jupiter and Saturn is a difficulty for the standard model of giant planet formation by core accretion (Hubickyj et al. 2005). The migration rate depends on the distribution of gas near the planet, which can be altered by magnetic forces (Terquem 2003). The midplane magnetic pressure in our calculations reaches a few percent of the gas pressure, sufficient for radial variations to halt or reverse the orbital migration. The outer edge of the undifferentiated zone is a plausible location for radial magnetic gradients large enough to stop the migration, and magnetic effects are a potential solution to the problem of the rapid loss of planetary embryos through migration.

An important question for future studies is how the mass flow rate varies with the distance from the star. The fraction of the column coupled to the magnetic fields generally increases with the radius. Possibly the inflowing gas will pile up at some location, leading to the development of a local radial pressure maximum (Kretke & Lin 2007). If so, gas drag forces push solid particles toward the maximum, providing favorable conditions there for the growth of planetesimals (Haghighipour & Boss 2003). The further build-up of material could lead to self-gravitational instability and an episode of rapid accretion on the star (Gammie 1996; Armitage et al. 2001) similar to those associated with intervals of strong mass outflow from young stellar objects (Reipurth 1989).

Part of this work was carried out at the Jet Propulsion Laboratory, California Institute of Technology using the JPL Supercomputing Facility and with support from the JPL Research and Technology Development and NASA Solar Systems Origins Programs.

## REFERENCES

Armitage P. J., Livio M. & Pringle J. E. 2001, MNRAS, 324, 705

Balbus S. A. & Hawley J. F. 1991, ApJ, 376, 214

Blaes O. M. & Balbus S. A. 1994, ApJ, 421, 163

Blandford R. D. & Payne D. G. 1982, MNRAS, 199, 883

Brandenburg A., Nordlund Å., Stein R. F. & Torkelsson U. 1995, ApJ, 446, 741

Brownlee D. et al. 2006, Science, 314, 1711

Ciesla F. 2007, ApJ, 654, L159

Cisowski S. M. & Hood L. L., in “The Sun in Time”, ed. C. P. Sonett, M. S. Giampapa & M. S. Matthews (Tucson: Univ. of Arizona Press), 761

Dullemond C. P. & Dominik C. 2005, A&A, 434, 971

Fleming T. & Stone J. M. 2003, ApJ, 585, 908

Fromang S., Terquem C. & Balbus S. A. 2002, MNRAS, 329, 18

Gammie C. F. 1996, ApJ, 457, 355

Garmire G., et al. 2000, AJ, 120, 1426

Goldreich P. & Tremaine S. 1979, ApJ, 233, 857

Haghighipour N. & Boss A. P. 2003, ApJ, 583, 996

Haisch K. E. Jr., Lada E. A. & Lada C. J. 2001, ApJ, 553, 153

Hartmann L., D’Alessio P., Calvet N. & Muzerolle J. 2006, ApJ, 648, 484

Hawley J. F., Gammie C. F. & Balbus S. A. 1995, ApJ, 440, 742

Hayashi C., Nakazawa K. & Nakagawa Y., in “Protostars and Planets II”, ed. D. C. Black & M. S. Matthews (Tucson: Univ. of Arizona Press), 1100

Hubickyj O., Bodenheimer P. & Lissauer J. J. 2005, Icarus, 179, 415

Igea J. & Glassgold A. E. 1999, ApJ, 518, 848

Ilgner M. & Nelson R. P. 2006, A&A, 445, 205

Inutsuka S. & Sano T. 2005, ApJ, 628, L155

Kretke K. A. & Lin D. N. C. 2007, ApJ, 664, L55

Miller K. A. & Stone J. M. 2000, ApJ, 534, 398

Nakagawa Y., Nakazawa K. & Hayashi C. 1981, Icarus, 45, 517

Parker E. N. 1993, ApJ, 408, 707

Reipurth B. 1989, Nature, 340, 42

Sano T., Miyama S. M., Umebayashi T. & Nakano T. 2000, ApJ, 543, 486

Sano T. & Stone J. M. 2002, ApJ, 577, 534

Stepinski T. F. 1992, Icarus, 97, 130

Stone J. M. & Norman M. L. 1992, ApJ, 80, 791

Stone J. M., Hawley J. F., Gammie C. F. & Balbus S. A. 1996, ApJ, 463, 656

Terquem C. E. J. M. L. J. 2003, MNRAS, 341, 1157

Turner N. J., Sano T. & Dziourkevitch N. 2007, ApJ, 659, 729

Ward W. R. 1997, Icarus, 126, 261

Wardle M. & Königl A. 1993, ApJ, 410, 218

Wardle M. 2007, Ap&SS, 311, 35